

Article

# Sea Surface Temperature Changes Reflected by Diatoms in the P6-10 Core from 1893 to 2013 from Prydz Bay, Antarctica

Yue Huang<sup>1,\*</sup>, Ruiwen Ma<sup>1</sup>, Jie Li<sup>2</sup> and Shuyu Tu<sup>1</sup>

<sup>1</sup> School of Earth Sciences, Yunnan University, Kunming 650500, China; maruiwen@itc.ynu.edu.cn (R.M.); shuyutu@163.com (S.T.)

<sup>2</sup> Yunnan Key Laboratory of Pollution Process and Management of Plateau Lake-Watershed, Yunnan Research Academy of Eco-Environmental Sciences, Kunming 650034, China; lijie@yreaes.org.cn

\* Correspondence: yuehuang@ynu.edu.cn

**Abstract:** Identification and analysis was conducted on the diatoms from the 19 cm sediment of the P6-10 core, drilled from China's 29th Antarctic Expedition, to attempt to semi-quantitatively reconstruct the annual sea surface temperature (SST) of Prydz Bay from 1893 to 2013. There were 30 species within the 12 genera of diatoms found, and the main contributors were *Fragilariopsis curta*, *F. cylindrus*, *F. sublinearis*, *F. ritscheri*, and *Thalassiosira antarctica*. They were divided into three categories based on their ecological affinity. The percentages of four specific species, i.e., *F. curta*, *F. cylindrus*, *F. ritscheri*, and *F. separanda*, which might be low SST indicators, were added together to represent the SST of Prydz Bay. With the help of cluster analysis, diatom assemblages were divided into diatom zones. Therefore, SST changes were divided into five stages by both the percentage of those four diatom species and the diatom zones: the high-temperature stage from 1893 to 1903, the cooling stage from 1903 to 1936, the stable and warm stage from 1936 to 1983, the low-temperature stage from 1983 to 1996, and the temperature rising stage from 1996 to 2013. On the multidecadal scale, SST change was affected by adjustments to solar radiation. On the contrary, the ENSO events mainly affected SST on the interannual scale. In addition, regarding the unique geographical environment (such as regional atmospheric circulation and a wind field) in Prydz Bay, volcanic eruptions and the like also played important roles in some exceptional periods.

**Keywords:** diatom; SST; semi-quantitative reconstruction; Prydz Bay



**Citation:** Huang, Y.; Ma, R.; Li, J.; Tu, S. Sea Surface Temperature Changes Reflected by Diatoms in the P6-10 Core from 1893 to 2013 from Prydz Bay, Antarctica. *J. Mar. Sci. Eng.* **2023**, *11*, 1428. <https://doi.org/10.3390/jmse11071428>

Academic Editors: Agata Di Stefano, Rosanna Maniscalco and Giulia Bosio

Received: 11 May 2023

Revised: 12 July 2023

Accepted: 15 July 2023

Published: 17 July 2023



**Copyright:** © 2023 by the authors. Licensee MDPI, Basel, Switzerland. This article is an open access article distributed under the terms and conditions of the Creative Commons Attribution (CC BY) license (<https://creativecommons.org/licenses/by/4.0/>).

## 1. Introduction

Of its special geographical location and unique ecological, climatic, and natural environment, Antarctica is less affected by human activities, which makes it unique in global change research [1]. Therefore, it is advantageous to research changes in natural factors in Antarctica, which will provide references with which to further explore the effects of human activities on global climate change. In addition, the abundant marine sediments in the Antarctic oceans contain a large amount of information about changes in the palaeo-ocean environment, which may provide more accurate records for the reconstruction of the palaeo-climates and palaeo-environments.

Marine sediments are important components of the marine ecosystem that provide information on the evolution of the ocean in the past, reflect the long-time-sequenced changes of the palaeo-climate and palaeo-environment, and provide an important basis for the reconstruction of the ecological environment during the historical period and its future development [2]. The changes in the palaeo-environment can be reflected by the fossils of microbiota in sediments as a bioenvironmental proxy indicator due to their difficulty in decomposition and sensitivity to the environment. Among them, diatoms, as one of the most commonly used carriers of information about past environmental evolution, have unparalleled advantages in reconstructing the palaeo-climate and palaeo-environment.

A diatom is a kind of important microcellular alga with a wide range of species, quantities, and distribution. It is found in almost all waters, from the poles to the tropics, whether in lakes, offshore areas, or oceans. Due to their high sensitivity to the environment, diatoms have been significantly affected by some important environmental factors such as temperature, salinity, and nutrients, etc., and can respond quickly to changes in those factors [3]. In addition, diatoms have siliceous shells that are not easily dissolved and can be stored in sediments for a long time [4]. Therefore, diatoms can reflect the past environment [5] as an effective bioenvironmental proxy indicator and have important advantages in the research of climate and environmental reconstruction. Benefitting from the development of dating technology and core drilling technology [6,7], reconstruction of the palaeo-climate and the palaeo-environment based on diatoms has been widely used in lakes [8–10] and oceans [11–13] all over the world. In the lakes, the research includes water depth [14], salinity [15], pH [16], conductivity [17], and indicators such as nitrogen and phosphorus that reflect eutrophication [18–20]. Compared with freshwater environments such as lakes, marine environments are more complicated, and the environmental parameters of inversion are, accordingly, different. Therefore, the main focus is on sea level [21], temperature [22], and salinity [23] in the oceans.

Temperature is the most basic physicochemical index in the ocean. Sea surface temperature (SST) is a result of ocean heat, dynamic action, and air–sea interaction. The ocean transfers the stored heat to the atmosphere through air–sea heat exchange, driving atmospheric motion through thermal changes and affecting atmospheric circulation [24]. Due to an “amplifier” effect of the changes in the Antarctic region on global change, an SST change in Antarctica has an important effect on regional and global climate change, and researching its pattern is essential for research on global change [25]. Moreover, the South Pacific Index (SPI) indicates that there may be a teleconnection between this region and ENSO events [26]. The reconstruction of SST helps restore the palaeo-ocean environment and understand the history of regional temperature changes and even global climate changes [27].

In winter, Prydz Bay is covered with thick sea ice. On the contrary, it gradually begins to melt in summer, followed by a reduction in sea ice concentration. By February, most areas become open sea; however, some are still covered by floating ice [28,29]. As a seasonal sea ice region, there is high biomass under the ice sheet and in an ice edge region [30], which also makes diatoms diverse and abundant. Especially in summer, phytoplankton blooms [31]. Obvious glaciomarine sedimentation develops the sediments well and thick, making Prydz Bay an excellent region for the use of diatoms to reconstruct the palaeo-environment and a representative region for exploring the response and feedback of polar seas to the global change [32].

However, due to the limitation of sample age and resolution, research on reconstructing the palaeo-environment has mainly focused on medium and large timescales ranging from ten thousand to million years. For example, core diatom assemblages were divided into zones using diatoms, based on which eight stages had been divided over the past 15 ka, for a preliminary and semi-quantitative reconstruction of climate changes since the Late Pleistocene [33]. Quaternary diatom assemblages were analyzed, Quaternary sedimentation was explained [34,35], and the glacial environment in Prydz Bay had been reconstructed semi-quantitatively using diatoms [36]. Even more, some palaeo-climate and palaeo-environment indexes had also been reconstructed semi-quantitatively on a large timescale of one million years [37]. However, research on the small-scale reconstruction of the palaeo-environment in Prydz Bay over the past century remains relatively lacking.

A large number of surface and core sediments in Prydz Bay were successfully obtained in 2013 during China’s 29th Antarctic Expedition. Moreover,  $^{210}\text{Pb}$  dating of the cores showed that the timescale did not exceed 200 years, which provided massive and excellent sediment samples for research in Prydz Bay, especially for the small timescale reconstruction of climate and environmental changes in the last hundred years. In addition, much research on the diatom assemblages and their distribution has been carried out in Prydz Bay [34,38,39], which has also provided a steady foundation for the reconstruction

of palaeo-environment research over the past century. Therefore, based on the sediments in the P6-10 core extracted from Prydz Bay in 2013, this paper attempts to conduct a semi-quantitative reconstruction of SST on the last centennial scale and preliminarily discusses the relationship between regional sea environmental changes and the global change, which may provide some references for the research on the small timescale climate and environmental changes in Antarctica through diatoms.

## 2. Geographical Setting

Prydz Bay, located in East Antarctica, is deeply embedded in the Antarctic continent in a shape of an inverted triangle; moreover, it is the third largest bay in Antarctica [40]. The Amery Ice Shelf at the end of Lambert Glacier to the south, extending northward, is closely adjacent to Prydz Bay, with Princess Elizabeth Land to the east and Mac. Robertson Land to the west [35]. Two shoals have developed at the mouth of the bay, with the Four Ladies Bank to the northeast and the Fram Bank to the northwest. There is a waterway with a depth of about 600 m between them, which is an important channel for material and energy exchange between Prydz Bay and open oceans [41]. In addition, Prydz Bay is a main drainage channel for the Emery–Lambert Glacier, a trough valley zone where the downdraft of an ice sheet converges [42] and the wind speed is constantly increasing and deflecting to the left under the action of gravity, Coriolis force, and friction. The adjacent Antarctic continent along the coast of Prydz Bay has a low temperature, and the temperature in the bay is higher due to the effect of the warm and humid air in low latitudes, thereby resulting in a large temperature gradient along the coast of Prydz Bay [43]. Due to a thermal difference between the sea and the land, sea and land wind is easily generated in a transition zone around the Antarctic continent.

Water masses in Prydz Bay and its adjacent water mainly include Antarctic surface water (AASW), Antarctic bottom water (AABW), circumpolar deep water (CDW), and shelf water (SW) [44]. There is a clockwise eddy in the west-central part of the bay, the Prydz Gyre (PG), which is relatively closed; however, its water mass plays a limited role in Prydz Gyre activity [45]. The Antarctic coastal current (CoC) flowing from east to west originates from a cold water mass of the West Wind Drift [45]. It flows from the West Ice Shelf into the bay, passes the Amery Ice Shelf and Cape Darnley, and continues westward out of the bay [46]. The Antarctic circumpolar current (ACC) in the northern sea is mainly composed of a warm water mass called Circumpolar Deep Water (CDW). This rises to the surface at 67° S, and the modified circumpolar deep water (mCDW) enters Prydz Bay [46]. Another large cyclonic vortex, the Antarctic Divergence (AD), forms between the west-to-east Antarctic circumpolar current (ACC) and the east-to-west Antarctic slope current (ASC) [45].

## 3. Materials and Methods

### 3.1. Sampling

Diatoms were studied in the multi-tube core P6-10 (75.57° E, 68° S) in Prydz Bay, Antarctica (Figure 1), which was drilled by the “Snow Dragon” polar exploration vessel on 7 February 2013, during China’s 29th Antarctic Expedition. The sediment core is 19 cm thick and has a silty texture with little sand and no gravel. It is mainly composed of plankton remains, with very few land-based materials, and is bluish-gray in color. This core was divided into 19 samples on the deck of the exploration vessel. Each sample represented a 1 cm thick slice of sediment. The samples were stored in a 4 °C geological sample bank specially set up on the exploration vessel. Then, the samples were stored in the hydro-chemical analysis laboratory at the School of Earth Sciences at Yunnan University after the exploration vessel returned to China. The samples were stored in brown glass bottles sealed away from light after drying, grinding, and other pretreatments in the laboratory. A total of 19 continuous sediment samples covering a time interval of 120 years were identified and analyzed for diatom contents.

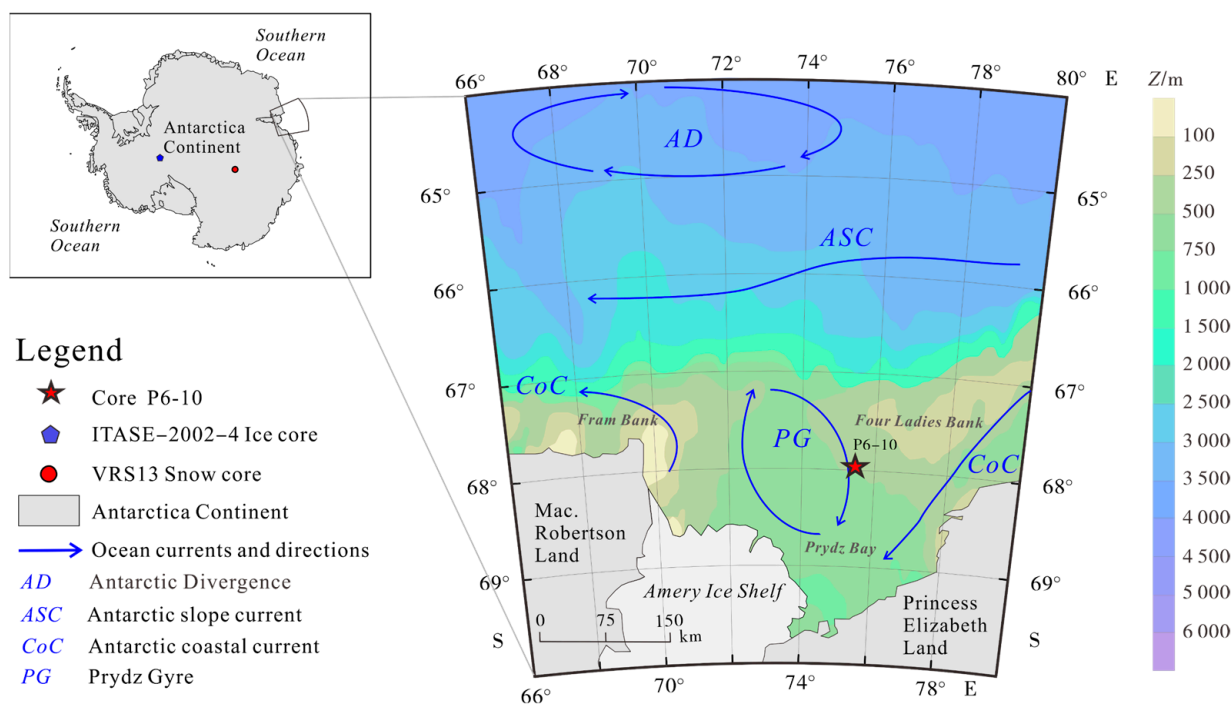


**Figure 1.** Schematic diagram of Prydz Bay with the position of the P6-10 core.

### 3.2. Treatment and Analysis of Diatoms

All the diatom samples were prepared as follows [47]: (1) 3–5 g of the sediment was dried and placed in a test tube; then, hydrochloric acid with a concentration of 10% was added (1 h) for uniform stirring to remove calcium, and the resultant was left for still standing for 12–24 h and cleaned with distilled water 3 times; (2) hydrogen peroxide with a concentration of 30% was added to remove organic material; the sample and the hydrogen peroxide were preliminarily reacted; the resultant was placed in a water bath (at 70 °C) for heating for 1–2 h; after the reaction was completed, the sample was taken out of the water bath, cleaned 3 times with distilled water again, and centrifuged (2500 rpm, 5 min) to remove water; (3) anhydrous ethanol was added for uniform stirring with a glass rod; then, a diatom suspension was smeared evenly on a coverslip with the glass rod; after it completely dried, Naphrax ( $d_n = 1.73$ ) was used to mount.

A Leica microscope with a magnification of  $\times 1000$  under oil immersion with phase contrast was used for identification. Diatoms were counted in random transects. More than 300 valves of diatoms were counted in each sample, and the percentage of each diatom species was measured. All diatoms were identified at the species level (excluding the *Chaetoceros* resting spores) according to diatom taxonomic references [48–51].

### 3.3. Age Model

$^{210}\text{Pb}$  dating of the P6-10 core was tested by the Second Institute of Oceanography, Ministry of Natural Resources, Hangzhou. A GWL-120-15N high-purity germanium gamma spectrometer produced by ORTEC was used along with the constant initial concentration (CIC) model. The results showed that the average sedimentation rate of the core is  $0.15 \text{ cm}\cdot\text{year}^{-1}$ , which spans from 1893 to 2013 C.E. (Figure 2).

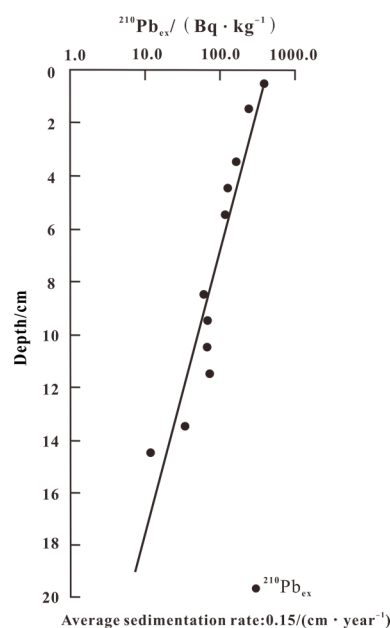


**Figure 2.**  $^{210}\text{Pb}$  profiles of the P6-10 core.

### 3.4. Cluster Analysis

Diatom assemblage zoning can be used to explain the characteristics of the diatom assemblages in different periods and the related ecological environment changes. Cluster analysis is a common ecological research method that is used to divide diatom zones. Stratigraphically constrained cluster analysis for numerical zonation provided by CONISS was used to cluster all the diatom species data in the sediment core due to the time continuity of the samples [52].

### 3.5. Semi-Quantitative Reconstruction

There are two key approaches to semi-quantitatively reconstructing the palaeo-environment based on diatoms: one is to use multivariate statistical analysis (such as canonical correspondence analysis (CCA)) to analyze the relationships between surface diatoms and environmental factors, finding the environmental factor most significantly affecting the composition and distribution of diatoms in the research region; meanwhile, the diatom with the strongest correlation with this environmental factor is selected as the corresponding environmental indicator species. The other is to analyze the composition of the diatoms in samples at different depths in the core sediment and to calculate a percentage sum of the diatom indicator species in each layer of samples. A change in the percentage sum of the diatom indicator species represents a change in the environmental factor. In combination with the  $^{210}\text{Pb}$  dating results, the change of the environmental factor over time is obtained to achieve a semi-quantitative reconstruction of a specific environmental factor. C2 1.4.2 software [53] is usually used to carry out the above operations.

## 4. Results

### 4.1. Diatom Assemblage

There were 30 species within the 12 genera of the diatoms found in the P6-10 core. *F. curta* (54.0% on average), *F. ritscheri* (11.2% on average), *Thalassiosira antarctica* (8.5% on average), *F. cylindrus* (5.7% on average), and *F. sublinearis* (4.2% on average) were the main contributors (Figure 3). Furthermore, the contents of some diatoms such as *F. separanda*, *F. kerguelensis*, *Porosira pseudodenticulata*, *Azpeitia tabularis*, and *Actinocyclus spiritus* were not dominant but also had important environmentally indicative significance. The percentages of some important diatom species are shown in Figure 3. The diatom assemblages can be divided into three categories: sea ice, ice edge, and cosmopolitan species. The original data of the diatoms are shown in Supplementary Materials Table S1.

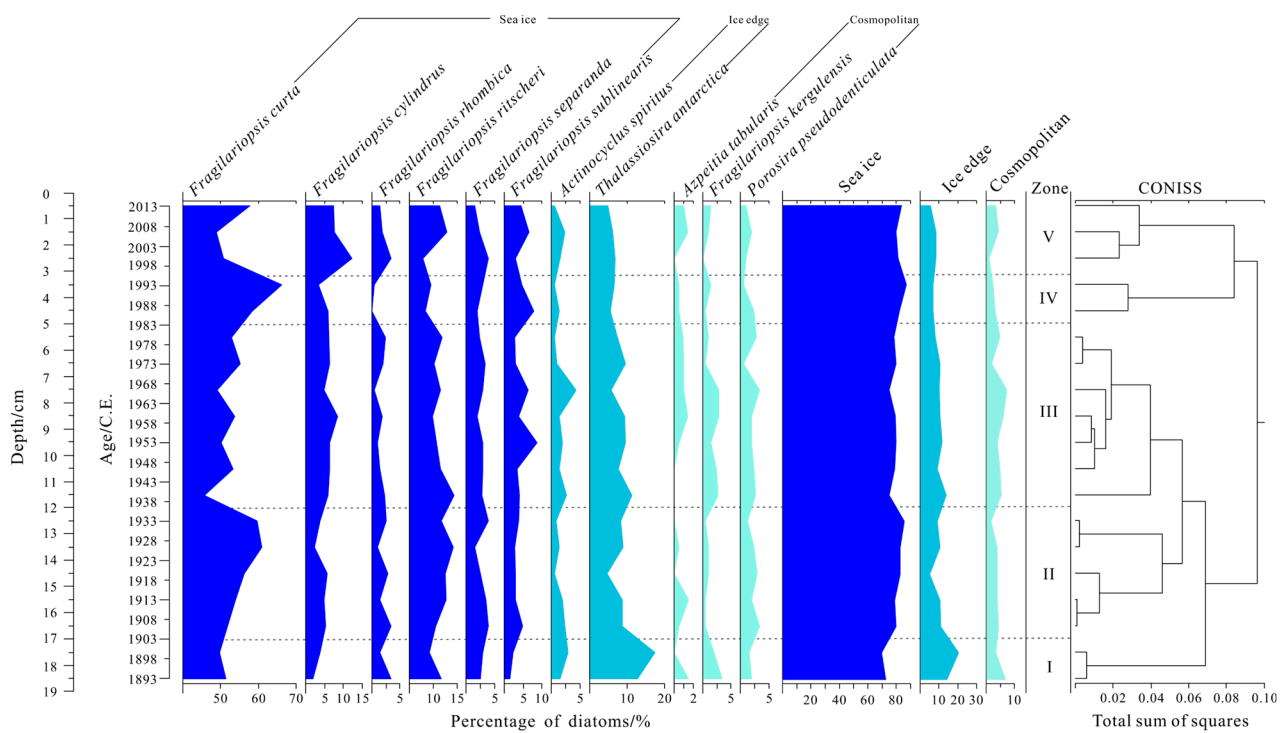


**Figure 3.** The percentage of some major diatoms in the P6-10 core.

#### 4.2. Ecological Affinity of Some Important Diatom Species in Prydz Bay

*F. kerguelensis*, *A. tabularis*, and *P. pseudodenticulata* are cosmopolitan species in terms of temperature. Among them, *F. kerguelensis* lives in relatively warm oceans [54] with a wide range of temperature adaptation and is considered eurythermic. *A. tabularis* is a typical species of tropical/subtropical diatoms that is found in sub-Antarctic regions and the Southern Ocean [50]; moreover, its maximum abundances is closely related to the warm SST [55]. *P. pseudodenticulata* is widely distributed in the oceans around Antarctica [48].

*T. antarctica* and *A. spiritus* frequently occur along the Antarctic coast or near the ice edge with a low SST; however, it is higher than the SSTs of typical sea ice species [48,56,57]. They are an ice edge species.

Although an endemic species in the Southern Ocean, *F. curta* is considered a relatively cold-living species. *F. cylindrus* is mostly distributed in high-latitude regions [58]. Its content is increased when there is a decrease in the SST, showing a good adaptation to the cold environment [59]. Therefore, it is often regarded as a sea ice indicator. *F. ritscheri* lives in the cold regions of Antarctic oceans with temperatures ranging from  $-1.6\text{ }^{\circ}\text{C}$  to  $-0.09\text{ }^{\circ}\text{C}$  [60]. In addition, *F. separanda* is also a common species found in Antarctic oceans that is related to the sea ice [61].

#### 4.3. Diatom Zones

According to the diatom assemblages in the samples at different depths, stratigraphically constrained cluster analysis for numerical zonation provided by CONISS was applied to analyze all the diatom species data in the P6-10 core. With a total sum of squares equal to 0.05 as a dividing line, five diatom zones were divided (Figure 3).

##### 4.3.1. Zone I (1893–1903 C.E. 17–19 cm)

The typical sea ice species *F. cylindrus* and *F. sublinearis* had the lowest abundance in this zone with percentages below 5%. Other sea ice species also had limited numbers. Comparatively, the percentage of the ice edge species *T. antarctica* reached its peak of 17.39%, and cosmopolitan species such as *F. kerguelensis* and *A. tabularis* also achieved their respective maximum contents. Overall, the percentage sum of the sea ice species

was the minimum in the five zones, and the percentage sum of the ice edge species was the maximum.

#### 4.3.2. Zone II (1903–1936 C.E. 12–17 cm)

This zone was divided into two sections in 1926. The percentages of some sea ice species such as *F. curta* and *F. ritscheri* showed a slowly increasing trend before 1926, and the abundance of ice edge species *A. spiritus*, *T. antarctica*, and some cosmopolitan species such as *P. pseudodenticulata* and *A. tabularis* were decreased. After 1926, *F. curta* and *F. ritscheri* reached peaks of 60.95% and 14.34% in the subsequent decade, respectively; moreover, most sea ice species in this period were at a relatively high level. However, the percentages of the three cosmopolitan species continued to decrease, and the percentage of *A. tabularis* even decreased to 0. Overall, the percentage sum of the sea ice species increased during this period, while the percentage sums of the ice edge and cosmopolitan species were decreased.

#### 4.3.3. Zone III (1936–1983 C.E. 5–12 cm)

Compared with the other four zones, the percentage changes of various diatoms in this zone were relatively stable. The percentages of the cosmopolitan species *P. pseudodenticulata*, *F. kerguelensis* and the ice edge species *A. spiritus* and *T. antarctica* were at a relatively high level. This period was divided into two sections based on data from 1968. The percentages of the sea ice species *F. curta*, *F. cylindrus*, and *F. sublinearis* and the cosmopolitan species *A. tabularis* increased, while the percentages of *F. ritscheri* and *F. rhombica* decreased before 1968. After 1968, sea ice species such as *F. separanda* and *F. sublinearis* decreased, while percentages of *F. curta*, *F. rhombica*, and two ice edge species increased. Overall, the percentage sum of the sea ice species in this zone was slightly lower, while the percentage sums of the ice edge species and the cosmopolitan species were higher.

#### 4.3.4. Zone IV (1983–1996 C.E. 3–5 cm)

The typical sea ice species *F. curta* was most abundant in this zone with a percentage above 50% and reached a peak of 66.19% in 1993. Other sea ice species such as *F. separanda* and *F. sublinearis* also reached a relatively high level. On the contrary, the percentage of the cosmopolitan species decreased, and *P. pseudodenticulata* reached its minimum percentage in 1993. Meanwhile, ice edge species such as *A. spiritus* and *T. antarctica* also had a low abundance. Overall, the percentage sum of the sea ice species in this zone gradually increased, while the percentage sums of the ice edge species and the cosmopolitan species gradually decreased.

#### 4.3.5. Zone V (1996–2013 C.E. 0–3 cm)

Most sea ice species had a relatively high amount of content in this zone, with *F. cylindrus*, *F. separanda*, and *F. rhombica* reaching their peaks of 12.32%, 3.94%, and 3.45%. Compared with Zone IV, the percentage of the sea ice species *F. curta* greatly decreased from 66.19% to 48.82%; therefore, the percentage sum of the sea ice species somewhat decreased, while the percentage of the ice edge species *A. spiritus* and three cosmopolitan species somewhat increased.

#### 4.4. Changes in SST Reflected by Specific Diatom Indicator Species

Based on previous research [62], 22 surface sediment samples and 6 environmental factors including the sea surface temperature were collected in the same cruise of the P6-10 core in 2013. A total of 29 species within 12 genera of diatoms were identified from the surface sediment samples, including 8 sea ice species. The exact relationship between the surface diatoms in Prydz Bay and environmental factors was analyzed using canonical correspondence analysis (CCA), and it was found that the sea surface temperature was the most important environmental factor affecting the composition and distribution of diatoms in the research region. In the CCA result diagram, the four diatoms, i.e., *F. curta*, *F. separanda*, *F. cylindrus*, and *F. ritscheri*, showed a strongly negative correlation with the

sea surface temperature, while the correlation between other sea ice species and the sea surface temperature was not strong. This indicated that not all ecological sea ice species can represent the low sea surface temperature in Prydz Bay and its adjacent water. Meanwhile, a large amount of *F. curta*, *F. separanda*, *F. cylindrus*, and *F. ritscheri* species were also identified in the P6-10 core. Therefore, we used these four sea ice species as low SST indicators to represent the low sea surface temperature in Prydz Bay (Figure 4).

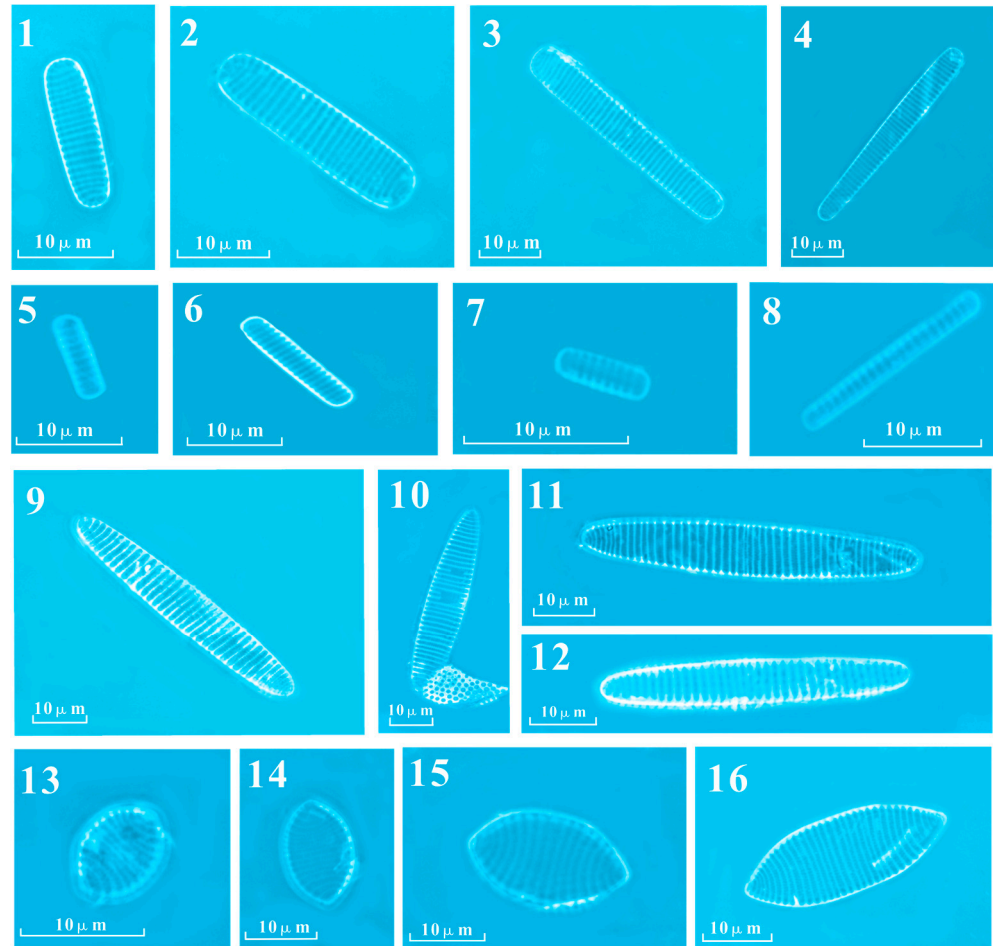


**Figure 4.** Plates of four specific diatom species representing low SST in Prydz Bay: (1–4): *F. curta*, (5–8): *F. cylindrus*, (9–12): *F. ritscheri*, (13–16): *F. separanda*.

In this paper, a change in the percentage sum of the four low SST diatom indicator species was used to reflect a change in the SST. A high percentage sum means that the sea surface temperature is low; the opposite means that the sea surface temperature is high. From this information, a semi-quantitatively reconstructed SST change curve is shown in Figure 5a. The sea surface temperature changes from 1893 to 2013 in Prydz Bay could be roughly divided into five stages: the high-temperature stage from 1893 to 1903, the cooling stage from 1903 to 1936, the stable and warm stage from 1936 to 1983, the low-temperature stage from 1983 to 1996, and the temperature rising stage from 1996 to 2013.

The percentage sum of the low SST diatom indicator species was about 68–72% from 1893 to 1903, which belonged to a low value stage in the research period. This means that the surface water was relatively warm during this period. The percentage sum of the low SST diatom indicator species was about 76% in 1993, which showed a slowly increasing trend in the following 30 years; by 1933, the percentage sum had reached about 85%. Over the next three years, the percentage sum further decreased slightly to about 80% in 1936. In general, the percentage sum of the low SST diatom indicator species increased during 1903–1936, while the sea surface temperature showed a decreasing trend. The percentage

sum of the low SST diatom indicator species from 1936 to 1983 fluctuated between 74% and 80%, and the overall change was little, reflecting the stable and warm stage. This period could be further divided into two stages: the sea surface temperature decreased slowly from 1936 to 1963 and then began to decrease again after a brief rise in 1963. The percentage sum of the low SST diatom indicator species increased from 80% in 1983 to 88% in 1993, indicating that the sea surface temperature decreased year by year during this period. The percentage sum of the low SST diatom indicator species decreased from 1996 to 2006 and increased after 2006 reflecting a general rising trend of the sea surface temperature.

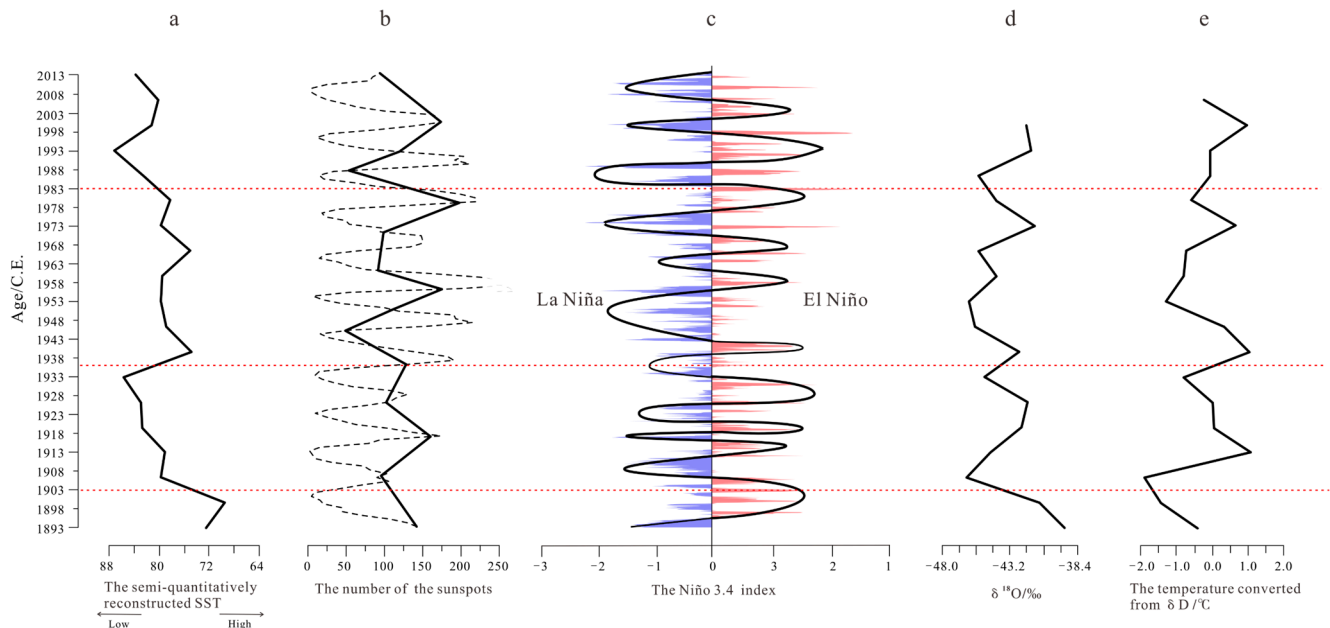


**Figure 5.** Comparison on a semi-quantitatively reconstructed SST with a number of sunspots, a Niño3.4 index, a  $\delta^{18}\text{O}$  in ice core ITASE-2002-4, and a temperature converted from  $\delta\text{D}$  of a snow core VRS13: (a) the semi-quantitatively reconstructed SST, (b) the number of the sunspots (a dotted line represents an original curve of the number of sunspots, and a solid line is a curve obtained after spline smoothing), (c) the Niño3.4 index (a solid black line represents the smoothed Niño3.4 index curve, a blue line represents La Niña events, and a red line represents El Niño events), (d)  $\delta^{18}\text{O}$ , and (e) the temperature converted from  $\delta\text{D}$ .

### 5. SST Reconstruction in Prydz Bay

Four types of records, which represent past temperature in the same timescale and were obtained from other research studies in Antarctica and the globe, were used to compare with the semi-quantitatively reconstructed SST in Prydz Bay. Sunspots are regarded as the primary indicator of solar activities, and the regularity of their periodic activities can affect the earth's climate change. Several of the sunspots herein are used to represent solar radiation intensity [63] (Figure 5b). The change in the global sea temperature is not isolated but rather synergistic. Abnormal SST signals of the ocean–atmosphere interaction in one sea area can be transmitted globally through atmospheric circulation, affecting the sea surface temperatures in other sea areas [64]. El Niño (La Niña) is a widespread and persistent abnormal warming (cooling) phenomenon of the sea surface temperatures in the eastern and central equatorial Pacific Ocean which can affect global climate change. The Niño3.4 index [65] herein is used to define El Niño and La Niña events (Figure 5c). Precipitations  $\delta\text{D}$  and  $\delta^{18}\text{O}$  are closely related to temperature and are the most widely used climate proxies; moreover, they can better indicate a change in the temperature [66]. Therefore, we used a  $\delta^{18}\text{O}$  record [67] (Figure 5d) of an ice core ITASE-2002-4 (86.5° S, 107.99° W, Figure 1) that described the atmospheric temperature in West Antarctica, as well as the temperature converted using a  $\delta\text{D}$  record [68] (Figure 5e) of a snow core VRS13 at

Vostok in East Antarctica (78.47° S, 106.83° E, Figure 1). In this chapter, the change in trends and causes of the sea surface temperature in the five stages are discussed.

#### 5.1. 1893–1903. C.E.

The semi-quantitatively reconstructed SST was relatively high in this period, indicating that Prydz Bay was in the high-temperature stage, in which the temperature steadily rose before 1900 [69]. The global temperature recorded in glaciers [70] and boreholes [71] all over the world also indicated the warming trend from 1890 to 1900. Then, the decreased semi-quantitatively reconstructed SST showed a short-term cooling period after 1900. The  $\delta^{18}\text{O}$  records [67] and the temperature converted from  $\delta\text{D}$  [68] also represented the same trend. Moreover, this was demonstrated by the number of sunspots that decreased from nearly 150 to 0 [63]. From 1895 to 1903, multiple El Niño events occurred consecutively [65], which might be the reason for the high temperature during this period.

#### 5.2. 1903–1936. C.E.

The SST showed a downward trend during this period. It started to decrease after 1900 and rose again from 1933 to 1936. The global sea surface temperature entered a relatively cold period after 1900 [24], and the SST estimated from  $\text{U}_{37}^{\text{K}}$  in Prydz Bay also showed a low temperature around 1904 [72]. The atmospheric temperature reflected by  $\delta^{18}\text{O}$  [67] rose for a short time between 1906 and 1913. On the contrary, the SST reflected by diatoms continued to decline, which might be due to the weakening of solar radiation reflected by the minimal number of sunspots [63]. Furthermore, the successively occurring La Niña events prolonged the abnormal cooling of the SST, resulting in a continuous decrease in the SST in the research region [65]. After 1935, a warming SST period occurred [24], which was also reflected by the  $\delta^{18}\text{O}$  [67] and  $\delta\text{D}$  [68] records. It was a warming period [73] that was affected by the rise in the radiation intensity of the sun.

#### 5.3. 1936–1983. C.E.

The semi-quantitatively reconstructed SST was higher in this stage. It was a relatively stable and warm period, as demonstrated by the global atmospheric temperature [73]. The SST continued to rise from 1936 to 1940, and the global temperature increased synchronously [73], with a peak occurring in 1940 [24]. Then, a slight decrease in the SST was occupied from 1946 to 1960, which was represented by both  $\delta^{18}\text{O}$  [67] and  $\delta\text{D}$  [68] data. The consecutive La Niña events that occurred between 1940 and 1953 resulted in the continuous cooling of the SST [65], which might explain the decrease in the SST in the research region during this stage. From 1966 to 1983, the SST gradually decreased, which showed the same trend as the SST estimated from  $\text{U}_{37}^{\text{K}}$  in Prydz Bay [72]. However, an opposite result was represented by both the  $\delta^{18}\text{O}$  [67] and  $\delta\text{D}$  [68] records, which might be due to a certain lag in the SST response to the atmospheric temperature. Prydz Bay is located near Lambert Glacier, being a trough valley zone where a descending airflow of the ice sheet converges. Under the combined action of descending wind affected by terrain factors and the sea–land wind under the control of a sea–land thermal difference, the atmospheric circulation and wind field around it are relatively complex. The temperature change is caused by heat transfer between the atmosphere, the land, and the oceans [74]. In addition, it is also at the edge of the cold polar high-pressure control area in the Antarctic continent, which is affected by warm and wet air in the north and the strong cold air in the mainland; moreover, sometimes, abnormal weather processes occur. A colder year is controlled by the strong cold airflow in the mainland, and a warmer year is affected by a circumpolar low pressure [75].

#### 5.4. 1983–1996 C.E.

During this period, the semi-quantitatively reconstructed SST was low, indicating that the SST in Prydz Bay was relatively cold. With the lowest value occurring in 1993, a significant decrease in the SST was observed from 1983 to 1993, which corresponded to

the increasing sea ice in East Antarctica along the coast [76]. And the SST increased from 1993 to 1996. The increasing sea ice might enhance the reflectivity of the sea surface and reduce heat absorption [77], which, in turn, reduced the SST. It was also reflected by a small number of sunspots [63]. The temperature records of Zhongshan Station and Davis Station, which are relatively close to Prydz Bay, also indicate that the temperature in 1993 was the lowest in decades [78–80]. One of the reasons for the low temperature was the small effect of cyclones with a large effect of continental cold high pressure [81].

In addition, the Pinatubo volcano in the Philippines erupted in June 1991, and the Hudson volcano in Chile erupted in August of the same year, which might be another reason for the low temperature in Prydz Bay in 1993. The volcanic ash emitted into the atmosphere during eruptions, which made the solar radiation scattered and weakened, also lowered the temperature [82]. The direct effect generated by a single volcanic eruption typically lasts for 1–2 years, leading to the cooling of the climate in the hemisphere and even the globe, and this is more pronounced in the polar regions [83,84]. The Hudson volcano is close to Antarctica, and materials immediately moved southward after its eruption. However, the Pinatubo volcano is far away in the Northern Hemisphere, and emission particles are transported in the stratosphere and are then required to be transported to the Antarctic atmosphere by aerosols to have an effect.

#### 5.5. 1996–2013 C.E.

The SST gradually increased during the period from 1996 to 2006, which was also shown by the  $U_{37}^k$  record [72]. Correspondingly, the El Niño events that occurred from September 2004 to February 2005 might be the cause of the SST rising [65]. However, the semi-quantitatively reconstructed SST decreased after 2006, corresponding to two consecutive moderate La Niña events between 2010 and 2012, called the “double dip” La Niña event, which caused a widespread cooling of the SST [85] and may have even affected the SST in the research region.

## 6. Conclusions

(1) There were 30 species within 12 genera of diatoms found in the P6-10 core. The main contributors were *F. curta*, *F. cylindrus*, *F. sublinearis*, *F. ritscheri*, and *T. antarctica*. Three categories were divided based on their ecological affinity.

(2) Four dominant sea ice diatoms, *F. curta*, *F. cylindrus*, *F. ritscheri*, and *F. separanda* were selected to represent the SST in Prydz Bay. From 1893 to 2013, five stages were divided: the high-temperature stage from 1893 to 1903, the cooling stage from 1903 to 1936, the stable and warm stage from 1936 to 1983, the low-temperature stage from 1983 to 1996, and the temperature rising stage from 1996 to 2013.

(3) Among the factors that affect the SST in Prydz Bay, solar radiation is the most important factor on the multidecadal scale. Contrarily, it is controlled by the ENSO events at the interannual scale. The alternating changes of El Niño and La Niña lead to an increase or decrease in the SST. In addition, regionally unique physical-geographical environments such as the atmospheric circulation and wind field in Prydz Bay, as well as volcanic eruptions, also play important roles in the temperature changes. Among them, the effects of the intensity of the solar radiation and the volcanic eruptions are global, and the ENSO events have an effect on the regional SST; meanwhile, the effects of atmospheric circulation and the wind field are local.

(4) The diatom records are effective palaeo-environmental carriers of SST data in Prydz Bay and reflect the palaeo-climatic changes over the past century, which serve as a scientific basis for research on the global change on small timescales.

In this paper, the SST of Prydz Bay from 1893 to 2013 was semi-quantitatively reconstructed based on the percentage sum of the low SST diatom indicator species; from this, a good result was obtained, which has provided a certain reference for the further exploration of the relationship between the marine environmental change in the sea area and the global change. However, a quantitative relationship between the percentages of

diatoms and the SST was not established in this research, and the obtained value was not an actual value of the SST. The SST of the sea area may be quantitatively reconstructed by establishing a diatom–SST transfer function in the future, and the change in the SST may further be analyzed in combination with more data.

**Supplementary Materials:** The following supporting information can be downloaded at: <https://www.mdpi.com/article/10.3390/jmse11071428/s1>, Table S1: Percentage of diatoms in the P6-10 core.

**Author Contributions:** Conceptualization, Y.H.; methodology, Y.H. and R.M.; validation, J.L.; formal analysis, R.M.; investigation, Y.H. and J.L.; resources, Y.H.; data curation, S.T.; writing—original draft preparation, R.M.; writing—review and editing, Y.H.; visualization, R.M. and S.T.; supervision, Y.H.; project administration, Y.H.; funding acquisition, Y.H. All authors have read and agreed to the published version of the manuscript.

**Funding:** This research was funded by the National Natural Science Foundation of China (No. 41966008).

**Institutional Review Board Statement:** Not applicable.

**Informed Consent Statement:** Not applicable.

**Data Availability Statement:** The data used to support the findings of this study are available from the corresponding author upon request.

**Acknowledgments:** A sincere thanks for the effort and support to all the scientists, crew, and laboratory technicians on the “Snow Dragon” polar exploration vessel during China’s 29th Antarctic Expedition. And we also thank the Chinese Arctic and Antarctic Administration and the Polar Research Institute of China.

**Conflicts of Interest:** The authors declare no conflict of interest.

## References

- Budd, W.F. Antarctica and global change. *Clim. Chang.* **1991**, *18*, 271–299. [[CrossRef](#)]
- Anderson, N.J.; Rippey, B.; Gibson, C.E. A comparison of sedimentary and diatom-inferred phosphorus profiles: Implications for defining pre-disturbance nutrient conditions. *Hydrobiologia* **1993**, *253*, 357–366. [[CrossRef](#)]
- José, A.P.; Kozlova, O.G.; Muhina, V.V. Distribution of diatoms in the surface layer of sediment from the Pacific Ocean. In *The Micropaleontology of the Oceans*; Funnell, B.M., Riedel, W.R., Eds.; Cambridge University Press: Cambridge, UK, 1971; pp. 263–269.
- Round, F.E.; Crawford, R.M.; Mann, D.G. *The Diatoms*; Cambridge University Press: Cambridge, UK, 1990.
- Smol, J.P.; Stoermer, E.F. *The Diatoms: Applications for the Environmental and Earth Sciences*; Cambridge University Press: Cambridge, UK, 2010.
- Mackereth, F.J.H. A short core sampler for subaqueous deposits. *Limnol. Oceanogr.* **1969**, *14*, 145–151. [[CrossRef](#)]
- Pennington, W.; Tutin, T.G.; Cambray, R.S.; Fisher, E.M. Observations on lake sediments using fallout <sup>137</sup>Cs as a tracer. *Nature* **1973**, *242*, 324–326. [[CrossRef](#)]
- Fritz, S.C.; Juggins, S.; Battarbee, R.W.; Engstrom, D.R. Reconstruction of past changes in salinity and climate using a diatom-based transfer function. *Nature* **1991**, *352*, 706–708. [[CrossRef](#)]
- Witak, M.; Hernández-Almeida, I.; Grosjean, M.; Tylmann, W. Diatom-based reconstruction of trophic status changes recorded in varved sediments of Lake Żabińskie (northeastern Poland), AD 1888–2010. *Oceanol. Hydrobiol. Stud.* **2017**, *46*, 1–17. [[CrossRef](#)]
- Narancic, B.; Saulnier-Talbot, É.; St-Onge, G.; Pienitz, R. Diatom sedimentary assemblages and Holocene pH reconstruction from the Canadian Arctic Archipelago’s largest lake. *Écoscience* **2021**, *28*, 347–360. [[CrossRef](#)]
- Huang, Y.; Jiang, H.; Sarnthein, M.; Knudsen, K.L.; Li, D. Diatom response to changes in palaeoenvironments of the northern South China Sea during the last 15,000 years. *Mar. Micropaleontol.* **2009**, *72*, 99–109. [[CrossRef](#)]
- Lopes, C.; Mix, A.C. North Pacific paleotemperature and paleoproductivity reconstructions based on diatom species. *Paleoceanogr. Paleoclimatol.* **2018**, *33*, 703–715. [[CrossRef](#)]
- Orme, L.C.; Crosta, X.; Miettinen, A.; Divine, D.V.; Husum, K.; Isaksson, E.; Wacker, L.; Mohan, R.; Ther, O.; Ikehara, M. Sea surface temperature in the Indian sector of the Southern Ocean over the Late Glacial and Holocene. *Clim. Past* **2020**, *16*, 1451–1467. [[CrossRef](#)]
- Brugam, R.B.; McKeever, K.; Kolesa, L. A diatom-inferred water depth reconstruction for an Upper Peninsula, Michigan, lake. *J. Paleolimnol.* **1998**, *20*, 267–276. [[CrossRef](#)]
- Yang, X.; Wang, S.; Kamenik, C.; Schmidt, R.; Shen, J.; Zhu, L.; Li, S. Diatom assemblages and quantitative reconstruction for paleosalinity from a sediment core of Chencuo Lake, southern Tibet. *Sci. China Ser. D Earth Sci.* **2004**, *47*, 522–528. [[CrossRef](#)]
- Finkelstein, S.A.; Bunbury, J.; Gajewski, K.; Wolfe, A.P.; Adams, J.K.; Devlin, J.E. Evaluating diatom-derived Holocene pH reconstructions for Arctic lakes using an expanded 171-lake training set. *J. Quat. Sci.* **2014**, *29*, 249–260. [[CrossRef](#)]

17. Ryves, D.B.; McGowan, S.; Anderson, N.J. Development and evaluation of a diatom-conductivity model from lakes in West Greenland. *Freshw. Biol.* **2002**, *47*, 995–1014. [[CrossRef](#)]
18. Hall, R.I.; Smol, J.P. A weighted-averaging regression and calibration model for inferring total phosphorus concentration from diatoms in British Columbia (Canada) lakes. *Freshw. Biol.* **1992**, *27*, 417–434. [[CrossRef](#)]
19. Dong, X.; Bennion, H.; Battarbee, R.; Yang, X.; Yang, H.; Liu, E. Tracking eutrophication in Taihu Lake using the diatom record: Potential and problems. *J. Paleolimnol.* **2008**, *40*, 413–429. [[CrossRef](#)]
20. Yue, H.; Ruiwen, M.; Hongbo, S.; Jie, L.; Shuyu, T. Centennial Lake Environmental Evolution Reflected by Diatoms in Yilong Lake, Yunnan Province, China. *Appl. Sci.* **2023**, *13*, 5288.
21. Jinpeng, Z.; Tomczak, M.; Witkowski, A.; Zia, Z.; Chao, L. A fossil diatom-based reconstruction of sea-level changes for the Late Pleistocene and Holocene period in the NW South China Sea. *Oceanologia* **2023**, *65*, 211–229. [[CrossRef](#)]
22. Cochran, U.; Neil, H. Diatom (<63µm) distribution offshore of eastern New Zealand: Surface sediment record and temperature transfer function. *Mar. Geol.* **2010**, *270*, 257–271. [[CrossRef](#)]
23. Jiang, H.; Knudsen, M.F.; Seidenkrantz, M.-S.; Zhao, M.; Sha, L.; Ran, L. Diatom-based reconstruction of summer sea-surface salinity in the South China Sea over the last 15,000 years. *Boreas* **2013**, *43*, 208–219. [[CrossRef](#)]
24. Leijuan, D.; Hongping, L. Analysis of global sea surface temperature variation. *Geospat. Inf.* **2013**, *11*, 29–31+45+11. (In Chinese)
25. Rintoul, S.R. The global influence of localized dynamics in the Southern Ocean. *Nature* **2018**, *558*, 209–218. [[CrossRef](#)] [[PubMed](#)]
26. Wangye, M.; Hongchun, P.; Lizong, W.; Haofan, M. Interannual variation patterns of sea surface temperature anomaly in the Southern Ocean. *Period. Ocean Univ.* **2022**, *52*, 26–33. (In Chinese)
27. Veizer, J.; Prokoph, A. Temperatures and oxygen isotopic composition of Phanerozoic oceans. *Earth-Sci. Rev.* **2015**, *146*, 92–104. [[CrossRef](#)]
28. Jiuxin, S.; Kentang, L. A review on studies of ice-ocean interaction in the East Antarctica. *Mar. Sci.* **1999**, *122*, 22–25. (In Chinese)
29. Hui, F.; Zhao, T.; Li, X.; Shokr, M.; Heil, P.; Zhao, J.; Zhang, L.; Cheng, X. Satellite-Based Sea Ice Navigation for Prydz Bay, East Antarctica. *Remote Sens.* **2017**, *9*, 518. [[CrossRef](#)]
30. Arrigo, K.R.; Perovich, D.K.; Pickart, R.S.; Brown, Z.W.; Dijken, G.L.; Lowry, K.E.; Mills, M.M.; Palmer, M.A.; Balch, W.M.; Bahr, F.; et al. Massive phytoplankton blooms under Arctic sea ice. *Science* **2012**, *336*, 1408. [[CrossRef](#)]
31. Haisheng, Z.; Zhengbing, H.; Jun, Z.; Peisong, Y.; Chuanyu, H.; Weiping, S.; Dan, Y.; Genhai, Z.; Bing, L.; Peter, H.-U.; et al. Phytoplankton and chlorophyll a relationships with ENSO in Prydz Bay, East Antarctica. *Sci. China: Earth Sci.* **2014**, *44*, 1701–1712. (In Chinese)
32. Liqi, C. *Research on Response and Feedback of Antarctic Region to Global Change*; China Ocean Press: Beijing, China, 2004; pp. 1–611. (In Chinese)
33. Shiguo, W.; Jun, L. Paleoclimatic evolution recorded in sediments of the Prydz Bay, Antarctica in 15,000 years. *Acta Oceanol. Sin.* **1998**, *20*, 65–73. (In Chinese)
34. Taylor, F.; McMinn, A. Late Quaternary diatom assemblages from prydz bay, eastern antarctica. *Quatern. Res.* **2002**, *57*, 151–161. [[CrossRef](#)]
35. Taylor, F.; Leventer, A. Late Quaternary palaeoenvironments in Prydz Bay, East Antarctica: Interpretations from marine diatoms. *Antarct. Sci.* **2003**, *15*, 512–521. [[CrossRef](#)]
36. Barbara, L.; Crosta, X.; Massé, G.; Ther, O. Deglacial environments in eastern Prydz Bay, East Antarctica. *Quatern. Sci. Rev.* **2010**, *29*, 2731–2740. [[CrossRef](#)]
37. Villa, G.; Lupi, C.; Cobianchi, M.; Florindo, F.; Pekar, S.F. A Pleistocene warming event at 1 Ma in Prydz Bay, East Antarctica: Evidence from ODP site 1165. *Palaeogeogr. Palaeocl.* **2008**, *260*, 230–244. [[CrossRef](#)]
38. Taylor, F.; McMinn, A.; Franklin, D. Distribution of diatoms in surface sediments of Prydz Bay, Antarctica. *Mar. Micropaleontol.* **1997**, *32*, 209–229. [[CrossRef](#)]
39. Linggang, T.; Xibin, H.; Yue, H.; Dong, X.; Yeping, B.; Qian, G.; Jianru, Z. Distribution of diatoms in surface sediments pf Prydz Bay and adjacent waters, Antarctica. *Mar. Geol. Quatern. Geol.* **2015**, *35*, 189–196. (In Chinese)
40. Rathburn, A.E.; Pichon, J.-J.; Ayress, M.A.; Deckker, P.D. Microfossil and stable-isotope evidence for changes in Late Holocene palaeoproductivity and palaeoceanographic conditions in the Prydz Bay region of Antarctica. *Palaeogeogr. Palaeocl.* **1997**, *131*, 485–510. [[CrossRef](#)]
41. O'Brien, P.E.; Cooper, A.K.; Florindo, F.; Handwerker, D.A.; Lavelle, M.; Passchier, S.; Pospichal, J.J.; Quilty, P.G.; Richter, C.; Theissen, K.M.; et al. Prydz channel fan and the history of extreme ice advances in Prydz Bay. *Proc. Ocean Drill. Program Sci. Results* **2004**, *188*, 1–32. [[CrossRef](#)]
42. King, J.C.; Turner, J. *Antarctic Meteorology and Climatology*; Cambridge University Press: Cambridge, UK, 1997.
43. Zhuoming, D.; Lin, Z.; Lingen, B.; Qizhen, S. Analysis of katabatic winds on the coast of Prydz Bay. *Chin. J. Polar Res.* **2015**, *27*, 351–363. (In Chinese)
44. Shuzhen, P.; Zhaoqian, D. Progress in physical oceanographic studies of Prydz Bay and its adjacent oceanic ares. *Chin. J. Polar Res.* **2003**, *15*, 53–64. (In Chinese)
45. Smith, N.R.; Zhaoqian, D.; Kerry, K.R.; Wright, S. Water masses and circulation in the region of Prydz Bay, Antarctica. *Deep Sea Res. Part I Oceanogr. Res. Pap.* **1984**, *31*, 1121–1147. [[CrossRef](#)]
46. Nunes Vaz, R.A.; Lennon, G.W. Physical oceanography of the Prydz Bay region of Antarctic waters. *Deep Sea Res. Part I Oceanogr. Res. Pap.* **1996**, *43*, 603–641. [[CrossRef](#)]

47. Håkansson, H. The recent diatom succession of Lake Havgårdssjön, south Sweden. In Proceedings of the Seventh International Diatom Symposium, Philadelphia, PA, USA, 22–27 August 1984; pp. 411–429.
48. Medlin, L.K.; Priddle, J. *Polar Marine Diatoms*; British Antarctic Survey: Cambridge, UK, 1990; pp. 1–214.
49. Hasle, G.R.; Syvertsen, E.E. Marine diatoms. In *Identifying Marine Phytoplankton*; Academic Press: San Diego, CA, USA, 1997; pp. 5–385.
50. Jousé, A.P. Species novae Bacillariophytorum in sedimentis fundi Oceani Pacifici et Maris Ochotensis Inventae. *Novit. Syst. Plant. Non Vasc.* **1968**, *5*, 12–21.
51. Hustedt, F. Die Kieselalgen Deutschlands Österreichs und der Schweiz unter Berücksichtigung der übrigen Länder Europas sowie angrenzender Meeresgebiete. In *L. Rabenhorst's Kryptogamen-Flora von Deutschland Österreich und der Schweiz, Band VII*; Otto Koeltz Science Publishers: Koenigstein, Germany, 1959; Volume 2, pp. 1–845.
52. Grimm, E.C. CONISS: A FORTRAN 77 program for stratigraphically constrained cluster analysis by the method of incremental sum of squares. *Comput. Geosci.* **1987**, *13*, 13–35. [[CrossRef](#)]
53. Juggins, S. C2 User Guide. In *Software for Ecological and Palaeoecological Data Analysis and Visualisation*; University of Newcastle: Newcastle upon Tyne, UK, 2003; pp. 1–69.
54. Cong, W.; Jinlian, W.; Gaowen, H.; Shaoying, F.; Lifeng, W.; Peixin, L. Distribution of diatom assemblages in the surface sediments near the King George Island and Elephant Island, Antarctica. *Acta Geosci. Sin.* **2018**, *39*, 657–665. (In Chinese)
55. Romero, O.E.; Armand, L.K.; Crosta, X.; Pichon, J.J. The biogeography of major diatom taxa in Southern Ocean surface sediments: 3. Tropical/Subtropical species. *Palaeogeogr. Palaeocl.* **2005**, *223*, 49–65. [[CrossRef](#)]
56. Hasle, G.R.; Heimdal, B.R. Morphology and distribution of the marine centric diatom *Thalassiosira antarctica* Comber. *J. Microsc.* **1968**, *88*, 357–369. [[CrossRef](#)]
57. Lihua, R. The Holocene Paleoclimate and Paleoceanography in the Northern North Atlantic. Ph.D. Thesis, East China Normal University, Shanghai, China, 2008. (In Chinese).
58. Zong, Y. Mid- and late-Holocene sea-level changes in Roudsea Marsh, northwest England: A diatom biostratigraphical investigation. *Holocene* **1997**, *7*, 311–323. [[CrossRef](#)]
59. Lihua, R.; Jianfang, C.; Haiyan, J.; Hongliang, L.; Yong, L.; Kui, W. The distribution of surface sediment diatoms in the Bering Sea and Chukchi Sea. *Chin. J. Polar Res.* **2012**, *24*, 15–23. (In Chinese)
60. Cefarelli, A.O.; Ferrario, M.E.; Almandoz, G.O.; Atencio, A.G.; Akselman, R.; Vernet, M. Diversity of the diatom genus *Fragilariopsis* in the Argentine Sea and Antarctic waters: Morphology, distribution and abundance. *Polar Biol.* **2010**, *33*, 1463–1484. [[CrossRef](#)]
61. Armand, L.K.; Crosta, X.; Romero, O.; Pichon, J.J. The biogeography of major diatom taxa in Southern Ocean sediments: 1. Sea ice related species. *Palaeogeogr. Palaeocl.* **2005**, *223*, 93–126. [[CrossRef](#)]
62. Ruiwen, M.; Yue, H. Diatoms in surface sediments of Prydz Bay, Antarctica and their relationship to environmental factors. *Adv. Mar. Sci.* **2023**, *41*. (In Chinese) [[CrossRef](#)]
63. SILSO, World Data Center. Sunspot Number and Long-Term Solar Observations, Royal Observatory of Belgium, On-Line Sunspot Number Catalogue 1893–2013. Available online: <http://www.sidc.be/SILSO/> (accessed on 12 March 2023).
64. Marjani, S.; Alizadeh-Choobari, O.; Irannejad, P. Frequency of extreme El Niño and La Niña events under global warming. *Clim. Dyn.* **2019**, *53*, 5799–5813. [[CrossRef](#)]
65. Rayner, N.A.; Parker, D.E.; Horton, E.B.; Folland, C.K.; Alexander, L.V.; Rowell, D.P.; Kent, E.C.; Kaplan, A. Global analyses of sea surface temperature, sea ice, and night marine air temperature since the late nineteenth century. *J. Geophys. Res.* **2003**, *108*, 4407. [[CrossRef](#)]
66. Jones, P.D.; Marsh, R.; Wigley, T.M.L.; Peel, D.A. Decadal timescale links between Antarctic Peninsula ice-core oxygen-18, deuterium and temperature. *Holocene* **1993**, *3*, 14–16. [[CrossRef](#)]
67. Steig, E.J.; Ding, Q.; White, J.W.C.; Küttel, M.; Rupper, S.B.; Neumann, T.A.; Neff, P.D.; Gallant, A.J.E.; Mayewski, P.A.; Taylor, K.C.; et al. Recent climate and ice-sheet changes in West Antarctica compared with the past 2000 years. *Nat. Geosci.* **2013**, *6*, 372–375. [[CrossRef](#)]
68. Ekaykin, A.A.; Kozachek, A.V.; Lipenkov, V.Y.; Shibaev, Y.A. Multiple climate shifts in the Southern Hemisphere over the past three centuries based on central Antarctic snow pits and core studies. *Ann. Glaciol.* **2014**, *55*, 259–266. [[CrossRef](#)]
69. Jian, L.; von Storch, H.; Xing, C.; Zorita, E.; Sumin, W. Long-time modeling experiment on global climate change for the last millennium. *Adv. Earth Sci.* **2005**, *20*, 561–567. (In Chinese)
70. Oerlemans, J. Extracting a climate signal from 169 glacier records. *Science* **2005**, *308*, 675–677. [[CrossRef](#)]
71. Huang, S.; Pollack, H.N.; Shen, P.-Y. Temperature trends over the past five centuries reconstructed from borehole temperatures. *Nature* **2000**, *403*, 756–758. [[CrossRef](#)]
72. Peisong, Y. Ocean Sediment Records and Their Responses to Climate Change in Prydz Bay, Antarctica. Ph.D. Thesis, University of Chinese Academy of Science (Institute of Oceanology), Qingdao, China, 2013. (In Chinese).
73. Bernstein, L.; Bosch, P.; Canziani, O.; Zhenlin, C.; Christ, R.; Davidson, O.; Hare, W.; Huq, S.; Karoly, D.; Kattsov, V.; et al. *Climate Change 2007: Synthesis Report*; Intergovernmental Panel on Climate Change: Valencia, Spain, 2007.
74. Mingjun, Z.; Zhongqin, L.; Dahe, Q.; Cunde, X.; Jiawen, R.; Jiancheng, K.; Jun, L. A study of climate and environment in Princess Elizabeth Land, Antarctica in the past 250 years. *Earth Sci. Front.* **2002**, *9*, 193–197. (In Chinese)

75. Xiaojun, T. Climatic change characteristics of Prydz Bay, Antarctica in the last 10 years. *Heilongjiang Meteorol.* **2006**, *51*, 20–22. (In Chinese)
76. Jinnian, C.; Jianting, C.; Lanying, X. Spatiotemporal characteristics of antarctic temperature and sea ice and their relationship. *Acta Oceanol. Sin.* **2003**, *25*, 39–47. (In Chinese)
77. Hao, M.; Zhaomin, W.; Jiuxin, S. The role of the Southern Ocean physical processes in global climate system. *Adv. Earth Sci.* **2012**, *27*, 398–412. (In Chinese)
78. Osborn, T.J.; Jones, P.D. The CRUTEM4 land-surface air temperature dataset: Construction, previous versions and dissemination via Google Earth. *Earth Syst. Sci. Data* **2014**, *6*, 61–68. [[CrossRef](#)]
79. Jones, P.D.; Lister, D.H.; Osborn, T.J.; Harpham, C.; Salmon, M.; Morice, C.P. Hemispheric and large-scale land-surface air temperature variations: An extensive revision and an update to 2010. *J. Geophys. Res. Atmos.* **2012**, *117*, D05127. [[CrossRef](#)]
80. Weigang, W.; Maifeng, W. Climatic characteristics and trends analysis of Zhongshan Station in Antarctica from 1990 to 2020. *Meteorol. J. Inn. Mong.* **2021**, *148*, 3–9. (In Chinese)
81. Shengli, H. Changes of weather system and meteorological elements of Zhongshan Station in Antarctica. *Mar. Forecast.* **2001**, *18*, 34–39. (In Chinese)
82. Zhengfu, G.; Jialin, L. Research advance in effect of volcanism on climate changes. *Adv. Earth Sci.* **2002**, *17*, 595–604. (In Chinese)
83. Ming, Y.; Dali, W.; Xiaoliang, L.; Dejun, T.; Yuansheng, L. Volcanism recorded in polar ice cores and its effects on climate. *Chin. J. Polar Res.* **2003**, *15*, 223–232. (In Chinese)
84. Fyfe, J.C. Southern Ocean warming due to human influence. *Geophys. Res. Lett.* **2006**, *33*, L19701. [[CrossRef](#)]
85. Feng, L.; Zheng, F.; Zhu, J.; Liu, H. The role of stochastic model error perturbations in predicting the 2011/12 double-dip La Niña. *Sola* **2015**, *11*, 65–69. [[CrossRef](#)]

**Disclaimer/Publisher’s Note:** The statements, opinions and data contained in all publications are solely those of the individual author(s) and contributor(s) and not of MDPI and/or the editor(s). MDPI and/or the editor(s) disclaim responsibility for any injury to people or property resulting from any ideas, methods, instructions or products referred to in the content.